Supplementary Information

Supplementary Figures

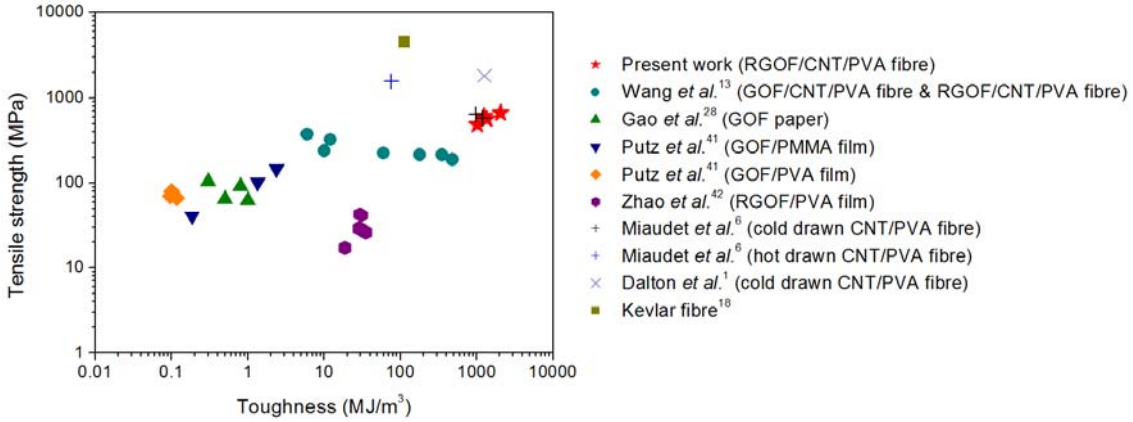

Supplementary Figure S1. Comparison of mechanical properties. Tensile strength versus toughness for various graphene-based materials and other reference materials. The red stars are values for the hybrid fibres made in this work.

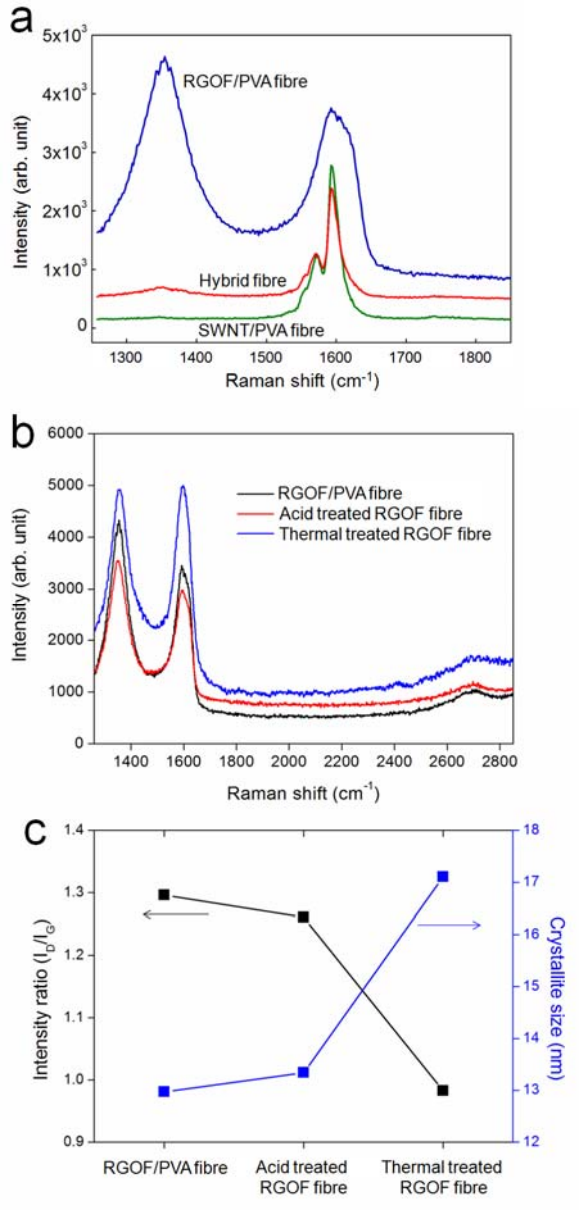

Supplementary Figure S2. Raman characterization of wet-spun fibres. (a) Raman spectra for carbon nanoparticles incorporated in 1:1 hybrid, SWNT/PVA, and RGOF/PVA fibres. **(b)** Raman spectra showing the D, G, and 2D bands of fibres containing RGOFs. **(c)** Graphs showing the ratios of D to G band intensities and the thereby calculated crystallite sizes (L_a) of RGOFs in solution spun fibres. The acid treated RGOF fibre and thermal treated RGOF fibre correspond to the RGOF fibre annealed at 600^{o} C to remove PVA and the RGOF fibre acid-treated (37% HCl) to remove PVA, respectively.

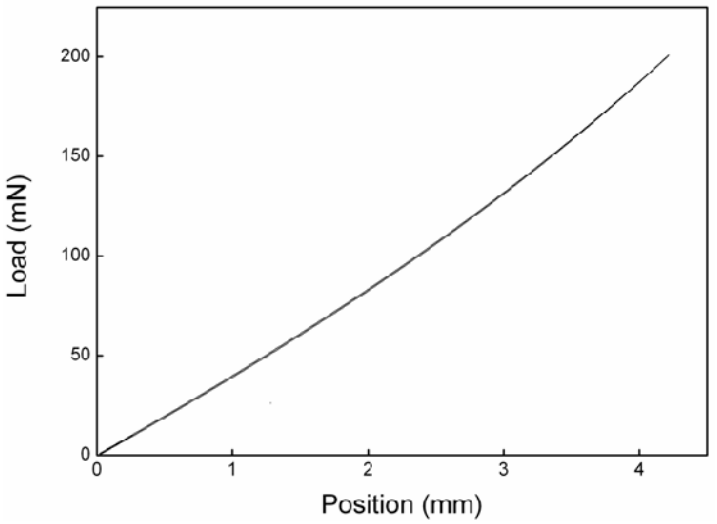

Supplementary Figure S3. Mechanical evaluation of a helical spring made from a 1:1 hybrid fibre. Force-displacement curve for a spring-shaped hybrid fibre made by setting the shape of a helically wound fibre at 150^{o} C. The spring constant derived from the slope of this curve is ~41 N/m.

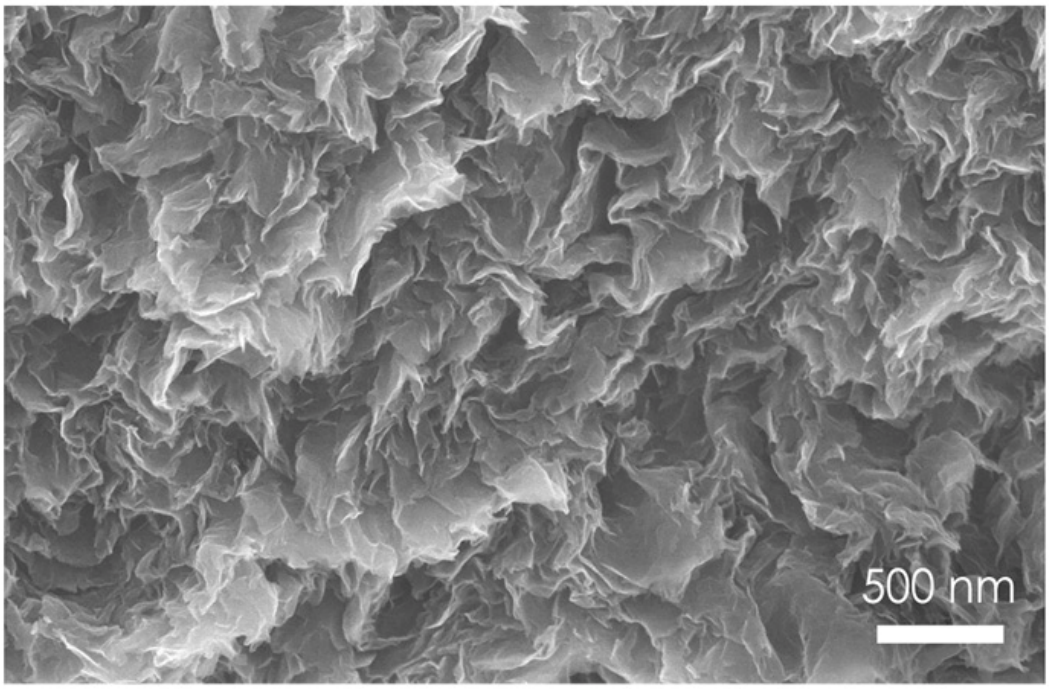

Supplementary Figure S4. Wrinkled RGOFs in fibres. SEM image showing the cross section of a RGOF fibre that has been annealed at 600 ^{o}C to remove the PVA.

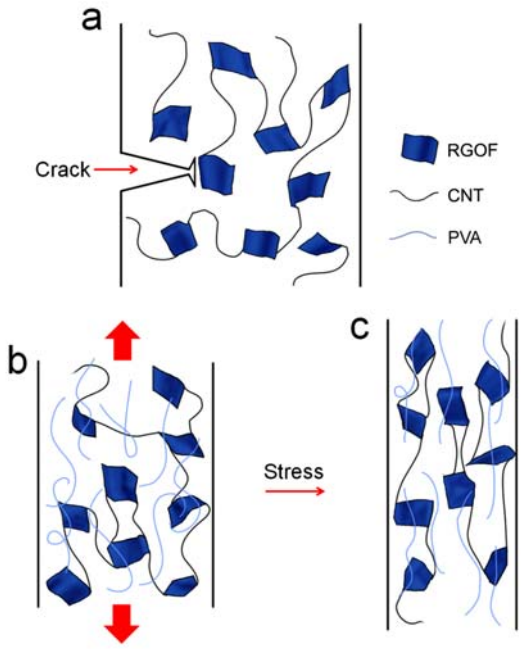

Supplementary Figure S5. Toughening mechanisms for hybrid fibres. (a) Picture illustrating crack deflection by a RGOF in a hybrid fibre. **(b, c)** Illustrations showing plastic deformation of the PVA matrix during tensile elongation: **(b)** partially aligned RGOFs and CNTs in a moderately oriented PVA matrix before substantial stretch and **(c)** highly aligned RGOFs and CNTs in a highly stretched fibre.

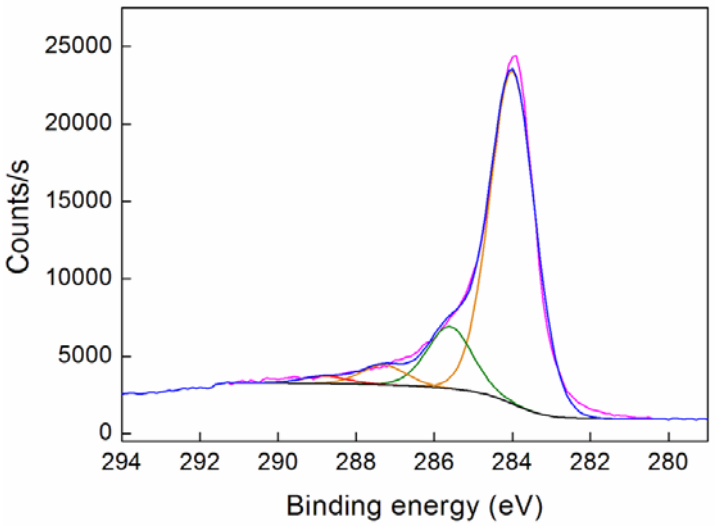

Supplementary Figure S6. Oxidation of RGOFs. XPS data for RGOFs. Carboxylate groups (O-C=O) provide binding energy peaks at 287.3 eV and 288.7 eV[43,44].

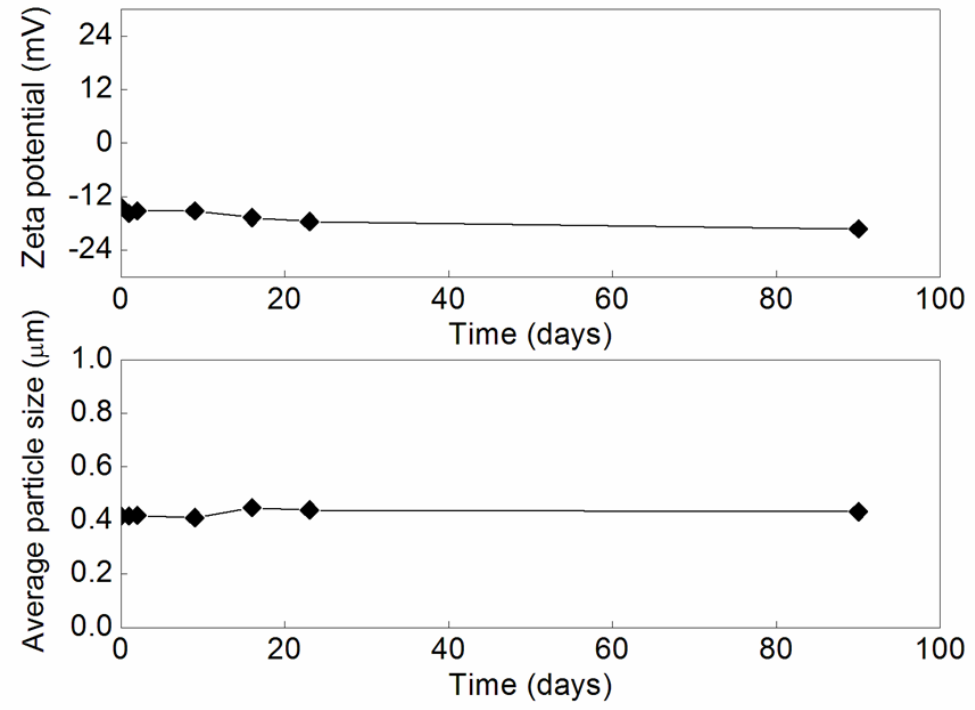

Supplementary Figure S7. Stability of RGOFs in DMF. Zeta potential (upper) and particle size (lower) measurements as a function of time for RGOFs dispersed in dimethylformamide.

Supplementary References

41. Putz, K. W., Compton, O. C., Palmeri, M. J., Nguyen, S. T. & Brinson, L. C. High-nanofiller-content graphene oxide–polymer nanocomposites via vacuum-assisted self-assembly. *Adv. Funct. Mater.* **20**, 3322–3329 (2010).

42. Zhao, X., Zhang, Q., Chen, D. & Lu P. Enhanced mechanical properties of graphene-based poly(vinyl alcohol) composites. *Macromolecules* **43**, 2357–2363 (2010).

43. Eda, G., Fanchini, G. & Chhowalla, M. Large-area ultrathin films of reduced graphene oxide as a transparent and flexible electronic material. *Nature Nanotech.* **3**, 270-274 (2008).

44. Xu, Y., Bai, H., Lu, G., Li, C. & Shi, G. Flexible Graphene Films via the Filtration of Water-Soluble Noncovalent Functionalized Graphene Sheets. *J. Am. Chem. Soc.* **130**, 5856-5857 (2008).